Epi-benthic megafaunal zonation across an oxygen minimum zone at the Indian continental margin.

William R. Hunter[1*]; Kazumasa Oguri[2]; Hiroshi Kitazato[2]; Zakir A. Ansari[3]; Ursula Witte[1].

[1] Oceanlab, University of Aberdeen, Newburgh, Aberdeenshire, AB41 6AA. United Kingdom. r01wh8@abdn.ac.uk*, u.witte@abdn.ac.uk.
Tel: +44(0)1224 274447. Fax: +44(0)1224 274402.

[2] Japan Agency for Marine-Earth Science and Technology, Natsushima 2-15, Yokosuka, Kanagawa 237-0061, Japan.

[3] National Institute of Oceanography, Dona Paula - 403 004, Goa, India

Corresponding Author.

Abstract.

The Arabian Sea oxygen minimum zone (OMZ) impinges upon the Indian continental margin at bathyal depths (150 – 1500 m) producing changes in ambient oxygen availability and sediment geochemistry across the sea floor. The influence of these environmental changes upon the epi-benthic megafaunal assemblage was investigated by video survey at six stations spanning the OMZ core (540 m), lower boundary (800 – 1100 m) and below the OMZ (2000 m), between September and November 2008. Structural changes in the megafaunal assemblage were observed across the six stations, through changes in both megafaunal abundance and lebensspuren (biogenic traces). Most megafauna were absent in the OMZ core (540 m), where the assemblage was characterised by low densities of fishes (0.02 – 0.03 m^{-2}). In the lower OMZ boundary, megafaunal abundance peaked at 800 m, where higher densities of ophiuroids (0.20 – 0.44 m^{-2}) and decapods (0.11 - 0.15 m^{-2}) were present. Total abundance declined with depth between 800 and 2000 m, as the number of taxa increased. Changes in the megafaunal assemblage were predicted by changes in abundance of seven taxonomic groups, correlated to both oxygen availability and sediment organic matter quality. Lebensspuren densities were highest in the OMZ boundary (800 – 1100 m) but traces of large infauna (e.g. echiurans and enteropneusts) were only observed between 1100 and 2000 m station, where the influence of the OMZ was reduced. Thus, changes in the megafaunal assemblage across the Indian margin OMZ reflect the responses of specific taxa to food availability and oxygen limitation.

Key Words.

Arabian Sea; Lebensspuren; Megafauna; Oxygen Minimum Zone; Video Survey.

1. Introduction.

Oxygen minimum zones (OMZs) are large, geologically stable, water bodies where dissolved oxygen levels fall persistently below 0.5 $ml.l^{-1}$ (22 $\mu mol.l^{-1}$) (Levin 2003). OMZs form in mid-water as a consequence of high primary productivity at the ocean surface and poor advective mixing of the water column. Where OMZs impinge upon the seafloor strong gradients in oxygen availability and organic matter flux are observed (Devol and Hartnett, 2001). At present, approximately 6 % of the continental margins (1.5 million km^2 of seafloor) experience permanent dysoxic conditions within OMZs (Helly and Levin, 2004) and this area is predicted to grow as a consequence of both anthropogenic changes in climate and ecosystem dynamics (Bakun and Weeks, 2004; Stramma et al., 2008).

One of the largest OMZs occurs in the Arabian Sea, where 285,000 km^2 of continental margin sea floor is impacted between depths of 150 to 1500 m (Cowie et al., 1999; Helly and Levin, 2004). Within this region sediments are characterised by a high organic carbon content (Cowie et al., 1999) and preservation of labile organic compounds such as amino acids, lipids and photosynthetic pigments (Smallwood et al., 1999; Vandewiele et al., 2009; Woulds and Cowie, 2009). Thus, the benthic environment can be described as food rich and oxygen deficient. The composition of the benthic community changes concomitantly with oxygen and organic matter availability across an OMZ, with bacteria, calcareous foraminifera and nematodes abundant in the OMZ core (Cook et al., 2000; Gooday et al., 2000; Schmaljohann et al., 2001; Stevens and Ulloa, 2008) and high densities of hypoxia tolerant metazoan macrofauna and megafauna characterising the OMZ boundaries (Wishner et al., 1990; 1995; Levin et al., 1991; Murty et al., 2009).

Epibenthic megafauna are defined as the animals occupying the sediment surface, which are large enough to be observable within a photograph or video image (usually > 1 cm in size (Grassle et al., 1975). Megafaunal assemblages are patchy but, when present, contribute significantly to benthic community biomass (Lampitt et al., 1986; Thurston et al., 1994), oxygen consumption (e.g., Piepenburg et al., 1995) and carbon demand (Christiansen et al., 2001; Renaud et al., 2007). Aggregations of megafauna

structure the marine benthos through physical disturbance of the sediment (e.g. Gallucci et al., 2008), predation upon meio- and macrofauna (e.g., Ambrose, 1993; Hudson and Wigham, 2003), and selective removal of labile organic matter from the sediment (e.g., Miller et al., 2000; Ginger et al., 2001). In the Arabian Sea and Eastern Pacific Oceans changes in the epi-benthic megafaunal assemblage are observed across OMZ impacted continental margins. Only physiologically versatile fish penetrate into the core regions of OMZs (Quiroga et al., 2009) but high densities of hypoxia tolerant ophiuroids and decapod crustaceans are characteristic of the organic matter rich boundary regions (Wishner et al., 1990; 1995; Smallwood et al., 1999; Murty et al., 2009; Sellanes et al., 2010). These taxa feed at multiple trophic levels (Jeffreys et al., 2009b) controlling both the quality and quantity of sedimentary organic matter (Smallwood et al., 1999; Jeffreys et al., 2009a). Therefore, changes in megafaunal distribution across an OMZ-impacted margin will have significant impacts upon wider ecosystem processes, such as organic matter recycling and burial.

Lebensspuren are the conspicuous traces left by both infaunal and epibenthic megafauna organisms at the seafloor (Kitchell et al., 1978) and can be used to predict bioturbation intensity (e.g., Turnewitsch et al., 2000; Wheatcroft, 2006). In addition, infaunal megafauna, such as enteropneusts (Mauviel et al., 1987) and echiurans (Ohta, 1984), are detectable by the traces they leave on the sediment surface. Therefore, lebensspuren provide valuable information about megafaunal activity, sediment reworking and the presence of large infauna, which cannot be directly acquired (e.g., Jones et al., 2007).

Photographic surveys are an effective method to investigate the distribution and abundance of deep-sea fauna and lebensspuren (Solan et al., 2003). However, spatial heterogeneity of megafaunal assemblages tends to negatively bias abundance estimates derived from photo-transect surveys. By providing images continuously over time, video survey techniques mitigate against this problem and produce density estimates that are comparable to a direct visual census of an area (Tessier et al., 2005). Still-images can subsequently be captured from the video allowing the size of individual organisms to be measured (e.g., Piepenburg et al., 1995; Christiansen et al., 2001).

Here, we describe the megafaunal assemblages at six stations spanning the core and lower boundary of the OMZ at the little explored Indian continental margin. We test two main hypotheses: a) megafaunal assemblage structure changes across an OMZ impacted margin; and b) the differences in the megafaunal assemblage are correlated with changes in ambient oxygen availability and sediment organic quality. The study identifies the key taxa responsible for changes in the megafaunal assemblages, and tests the correlations between their abundance, oxygen availability and sediment C:N ratio. Changes in the lebensspuren were used to describe both megafaunal activity and infaunal presence. Biomass of the two most abundant megafaunal taxa, the ophiuroids and decapod crustaceans, was estimated to allow changes in the megafaunal assemblage to be considered within the context of wider ecosystem processes (e.g., Christiansen et al., 2001; Renaud et al., 2007).

2. Materials & Methods

Between September and November 2008, a multi-national research expedition aboard the *R/V Yokosuka* (YK08-11) explored the biology and biogeochemistry of the Arabian Sea OMZ along two transects of the Indian continental margin. The deep-sea submersible *Shinkai 6500* (Japan Agency for Marine-Earth Science and Technology, 2007) made a total of 24 dives, at six stations across the OMZ (Fig. 1; Table 1), recording a total of 140 hours of video footage at the sea floor. Nineteen 10-minute visual surveys were drawn from the ~ 2 % of video footage that was deemed suitable for quantitative analysis. The mean area of seafloor covered in each survey ranged from 50 – 80 m^2, covering a 10 - 40 m depth range around the target depth.

2.1 Environmental Data

Environmental data were recorded during each dive by *Shinkai 6500*. Salinity, temperature and pressure were recorded by CTD (SBE 19, Sea-Bird Electronics, Inc.), and oxygen concentrations measured using an optical oxygen sensor (Optode 3830, Aanderaa Data Instruments) mounted upon the submersible. A two-step calibration procedure was carried out to obtain accurate oxygen concentration in low-oxygen environments. Firstly, oxygen concentrations were calculated from optode data

following the method outlined in the user manual, with a pressure compensation coefficient of 3.2 % per 1000 dbar (Uchida et al., 2008). Secondly, water samples at different oxygen concentrations were prepared by bubbling nitrogen through freshwater. Oxygen concentrations of the freshwater samples were simultaneously measured by the optode and by Winkler Titration and the relationship between these data determined by

Eq. 1: $$[O_2]_c = 1.1381 * [O_2]_r + 0.1665$$

where $[O_2]_c$ is the Winkler Titration calibrated oxygen concentration (μmol.l^{-1}), and $[O_2]_r$ is the oxygen concentration recorded by the optode. In the present study all oxygen measurements were calibrated according to this relationship. Accuracy of the instrument was assumed to be ± 1 μmol.l^{-1} at oxygen concentrations < 50 μmol.l^{-1} (A. Tengberg, *pers. comm.*).

Sediment was sampled at each station using 8.2 cm diameter push cores in order to quantify the sediment organic matter (OM) content, OM quality and porosity. Three replicate cores were obtained at all stations except T1 1100 m, where only one core could be obtained. Sediment samples from the surficial 1 cm of each core were homogenized and deep-frozen at -80 ^{o}C until they could be processed. The frozen sediment was sub-sampled into 5 g aliquots, lyophilised (-60^{o}C; -0.0001 mbar) and porosity determined based upon the change in volume and mass between wet and dry sediment (Breitzke, 2006). Sediments were acidified to remove inorganic carbon by addition of excess 1 mol.l^{-1} hydrochloric acid, incubated at 30 ^{o}C, for 24 hours in an acid fumed environment (Hedges and Stern, 1984) and dried to constant weight at 60 ^{o}C. Total organic carbon content (% TOC) and total nitrogen content (% TN) were determined by a Fisons Instruments NA 1500 micro-elemental analyser. These data were used to calculate C:N ratios for each sediment sample as a proxy of sediment organic matter quality (e.g., Hedges and Keil, 1995).

178 *2.2 Video Survey Technique*

179

180 Video footage recorded at the six stations was used to carry out a quantitative visual
181 survey of megafauna and lebensspuren. Replicate surveys, comprising five one-
182 minute counts spread across a 10 minute period, were conducted at each station.
183 Densities of megafauna and lebensspuren were recorded as individuals observed per
184 unit time, for every one minute time interval. Frame-grabs were taken during each
185 minute of surveyed footage and the video imaging package Image-J used to calculate
186 the width of the camera field of view (Table 1). Images were calibrated to a 20 cm
187 scale provided by four laser pointers incorporated into the *Shinkai 6500* camera
188 system. Megafaunal and lebensspuren abundances (m^{-2}) calculated for each one
189 minute count by

190

191 Eq. 2: $$D_{area} = D_{time} / (W_c * V_{min})$$

192

193 where D_{area} is the relative abundance per unit area (ind. m^{-2}), D_{time} is the relative
194 abundance per unit time (ind. min^{-1}), W_c is the width seabed in the camera field of
195 view (m) and V_{min} is the average velocity of the submersible (30.87 m min^{-1}). Mean
196 abundance values were then calculated for each ten minute period to mitigate against
197 spatial patchiness of the megafaunal assemblages and provide comparable measures
198 of relative abundance at each station.

199

200 Precision is a major issue with visual surveys (e.g., Kimmel, 1985; Sayer and
201 Poonian, 2007). In the present study, each replicate covers a large spatial area. This
202 accounts for the patchiness of megafauna but limits the taxonomic resolution of the
203 visual survey. Few megafaunal specimens were available for identification because
204 dive-time with the submersible was limited by other experimental work, and the *R/V*
205 *Yokosuka* was not equipped for trawling. The present study focussed upon quantifying
206 the abundances of 15 broad taxonomic groups. Further description of the megafaunal
207 assemblage was conducted using video frame-grabs, still images and opportunistic
208 samples (Table 2). Conspicuous lebensspuren were identified and assigned to five
209 groups, following Gaillard's (1991) English-language nomenclature (table 3).

210

211

2.3 Estimation of Megafaunal Biomass

Estimations of biomass were made for the two most abundant taxa, the ophiuroids and decapods crustaceans, in particular the aresteid and solenocerid shrimps (*Plesiopenaeus* spp. and *Solenocera* spp.). Seven hundred and forty frame grabs were captured randomly and blurred images, images with less than 30 % of the visible seafloor, and images with no visible scale subsequently removed. Image-J was used to measure the size of visible ophiuroids and decapod crustaceans, calibrated to the laser scale in each image

Ophiuroid size was measured as disc diameter (cm) across a sample of 86 individuals. Biomass of individual ophiuroids was then calculated using the size-weight relationship described by Piepenburg and Schmid (1996) and converted to wet weight, based upon a conversion factor of 12.08 (Gage, 2003). These were used to convert ophiuroid size to wet weight by

Eq. 3: $$W_w = (0.1507 * d^{2.488}) / 12.08$$

where W_w is the wet weight (in grams) and d is the disc diameter in centimetres. Decapod size was measured as carapace length (cm), for a sample of 97 individuals and converted to wet biomass using a size-weight relationship described by Barriga et al. (2009) as

Eq. 4: $$W_w = 0.00321 * L_c^{2.37026}$$

where W_w is the wet weight (in grams) and L_c is the carapace length of a given individual. These estimates allowed the biomass-frequency distributions of both ophiuroid and decapod populations within the OMZ to be made. Ophiuroid and decapod biomass were calculated for each station as the product of the median individual biomass of each taxon and respective abundances in each survey.

2.4 Data Analysis

Data analysis was conducted in R, using the *stat* (R Development Core Team, 2009), *MASS* (Venables and Ripley 2002), *vegan* (Oksanen et al., 2009) and *StatFingerprints* (Michelland and Cauquil, 2010) packages. Data were graphically explored to assess their fits to assumptions of homoscedacity (homogeneity of variance) and independence (Zuur et al., 2010). Multivariate dispersion of the data was formally tested using a randomisation test (1000 permutations), at a significance level of $p < 0.05$ (Anderson, 2006). The data violated the assumptions of homoscedacity and multivariate normality and so analysis preceded using robust multivariate techniques. Analysis of Similarities (ANOSIM) tested the significance of changes in the megafaunal assemblage across the six stations, using a Bray-Curtis dissimilarity matrix of the untransformed megafaunal data. Non-metric multidimensional scaling (nMDS) of the dissimilarity matrix provided a visual ordination of the similarities and differences in megafaunal structure between stations. Similarity Percentage Analysis (SIMPER) was used to further explore the data, identifying taxonomic groups that contributed highly to the observed change in megafaunal assemblage structure (Clarke, 1993). Correlation tests were used to investigate the strength and significance of relationships between the abundances of individual megafaunal taxa and changes in oxygen availability and the sediment C:N ratio, across the six survey stations, using the Spearman's rank coefficient (Spearman, 1904).

3. Results

3.1. Environmental Description

Temperature, salinity and oxygen profiles are shown in figure 2, and the environmental data at each survey station summarised in table 1. Oxygen concentrations increased along a depth-dependent gradient from 0.35 $\mu mol.l^{-1}$ at T1 540 m, to 136.00 $\mu mol.l^{-1}$ at T1 2000 m, exhibiting strong co-linear relationships with salinity and temperature (Fig. 3). Sediment organic carbon (% TOC) and nitrogen concentrations (% TN) were highest at the 800 and 1100 m stations, in the lower OMZ boundary, and lowest at the 2000 m station, below the OMZ. Both % TOC and

% TN exhibited co-linear relationships with sediment porosity, indicating positive correlations between accumulation of OM and the amount of pore space within the sediment. The sediment C:N ratios provide a proxy of OM quality derived from the % TOC and % TN. Within the OMZ, C:N ratios ranged between 8.38 at T2 1100 m and 9.72 at T1 540 m indicating small-scale diagenetic alterations of relatively labile sedimentary OM. Below the OMZ, at T1 2000 m, a C:N ratio of ~ 19.38 was indicative of refractory organic matter within the sediment. Thus, the C:N ratio is a useful proxy for the overall changes in sediment geochemistry across the six stations (Hedges and Keil, 1995).

Across the six stations, the described environmental conditions are reflected in the appearance of the seafloor (Fig 4.). Between 540 and 1100 m the seabed was typically composed of homogenous, fine grained sediments. Patches of sharp-crested ripples at station T1 540 m and slight rippling of the sediment surface at T1 800 m indicate that the sediment surface at the stations is disturbed by fairly rapid water movements. These ripples are indicative of currents, within the Indian margin OMZ, which may be linked to regional tidal cycles. Carbonate deposits were observed at the 1100 m stations and may provide important habitat complexity in this depth range.

3.2. Lebensspuren.

There were changes in both the density and variety of lebensspuren observed across the study area. No traces where observed at stations T1 540 m and T1 800 m, where oxygen levels were low. Patches of burrow openings were observed at stations T2 800 m and T1 1100 m. More varied lebensspuren were observed at T2 1100 m and T1 2000 m, characterised by low overall densities and the presence of hole-rings, star-like traces and scour traces (Fig. 5).

3.3 Megafaunal Assemblage Structure

The megafaunal assemblage exhibited significant structural variations between the six survey stations ($R = 0.78$; $p = 0.01$). The assemblage at T1 540 m was distinct from all other stations (800 – 2000 m), characterised by low abundances of fishes and the absence of invertebrate megafauna. Thus, comparatively little within-station variation

was observed at this station. In contrast, higher levels of within station variability and a gradual, depth-dependent increase in the number of taxonomic groups represented were observed between 800 and 2000 m (Table 4; Fig. 6).

SIMPER analysis (Appendix A & B) quantified the relative contributions of each taxon surveyed to the similarities within, and differences between, the megafaunal assemblages at each station. This analysis identified seven taxa that consistently contributed to either within station similarity or the differences between stations. These were the Actiniaria, Decapoda, Ophiuroidea, Asteroidea, Holothuroidea, Echinoidea and Gnathostomata (fishes). Each taxon exhibited a specific distribution pattern between stations, with most taxa found in high abundances between 800 m and 1100 m (Fig. 7). Peaks in ophiuroid and decapod abundance were features of the assemblage at the 800 m stations, and high densities of actiniarians and fishes were observed at the 800 and 1100 m stations. In addition, the 1100 m stations are characterised by the presence of echinoids and asteroids, absent at both 540 and 800 m.

Changes in the relative abundance of each taxon were correlated with changes in environmental conditions across the OMZ (Table 5). Abundance of most groups strongly correlated with sediment C:N ratios, but both the asteroids and echinoids were strongly correlated with oxygen availability. These correlations suggests that both oxygen and organic matter availability influence megafaunal assemblage structure across the six stations.

3.4 Ophiuroid and Decapod Biomass.

Biomass-frequency distributions of both the ophiuroids and decapod crustaceans, across the six survey stations were negatively skewed (Appendix C). Over 70 % of the ophiuroids sampled were estimated to have wet weights < 2 g, with no individual > 11 g, and most individual decapods (75 -85 %) had estimated weights < 100 g. Biomass of both the ophiuroids and decapods peaked at the 800 m station, declining with depth between 800 and 2000 m (Fig. 8). The decapods exhibited substantially higher biomass than the ophiuroids, across all stations where these megafauna were

present. However, the ophiuroids exhibited a greater relative change in biomass across the study area.

4. Discussion

The present study investigated changes in the epi-benthic megafaunal assemblages between 540 m and 2000 m on the Indian continental margin, and how these were influenced by differences in oxygen availability and sediment organic matter quality across the OMZ. The megafaunal assemblage changed significantly across the study area. Fish dominated the assemblage in the OMZ core (540 m), but in the lower OMZ boundary high densities of ophiuroids and decapods produced megafaunal abundance peaks at 800 m, below which total faunal abundance declined gradually with depth. Abundances of individual faunal groups correlated significantly with either ambient oxygen availability or the sediment C:N ratio. These results are consistent with previous studies on the Pakistan margin (Murty et al., 2009) and in the eastern Pacific (Wishner et al., 1990; 1995; Quiroga et al., 2009; Sellanes et al., 2010), suggesting that megafaunal assemblage structure is determined by the responses of individual taxa to limitation of two resources, oxygen and sediment organic matter.

4.1.Megafaunal assemblage structure.

On the Indian continental margin there are changes both in megafaunal abundance and assemblage structure across the OMZ. These broadly correspond to the zonation pattern implicit in the biofacies model of Levin et al. (1991), evidenced by the presence of only hypoxia-tolerant fishes in the OMZ core (540 m; $[O_2]$ = 0.35 μmol.l^{-1}) compared with high abundances of invertebrate megafauna and lebensspuren across OMZ boundary (800 – 1100 m; $[O_2]$ = 2.20 – 15.00 μmol.l^{-1}). Below the OMZ (2000 m; $[O_2]$ = 163.00 μmol.l^{-1}) a larger number of megafaunal taxa were present and the lebensspuren featured echiuran and enteropneust traces alongside scours indicative of bioturbation by fishes and large crustaceans (Gaillard, 1991). Thus, the results indicate that variability in both the megafaunal assemblage and lebensspuren increases along the depth-dependent oxygen gradient.

377 The absence of the invertebrate megafauna at the OMZ core is striking. Carcasses
378 decay slowly in OMZ-impacted margins (Billett et al., 2006) and well preserved
379 remains of large fish and cephalopods were observed at station T1 540 m (U. Witte &
380 H. Kitazato, *pers. obs.*). This station should represent an ideal foraging ground for
381 scavengers. However, typical scavenging fishes, e.g. macrourids and zoarcids, and
382 invertebrates, e.g. lysianassid amphipods and *Plesiopenaeus* spp. shrimps (Witte,
383 1999) were absent at the observed carcasses. Instead a resident fish fauna, which
384 included representatives of the families Liparidae (W.R. Hunter, *pers. obs.*) and
385 Gobiidae (L. Levin, *pers. comm.*), was observed. Murty et al., (2009) suggests that
386 these fish are migratory, utilising the hypoxic waters as a refuge from predation.
387 However, a permanent fish fauna characterises the core of OMZs in the Eastern
388 Pacific (e.g., Quiroga et al., 2009), suggesting adaptation to these habitats. The
389 presence of fishes with the OMZ may therefore be a product of both predation and
390 disturbance release, rather than the provision of refuge.
391
392 A modal shift in megafaunal assemblage structure occurs between 540 and 800 m
393 ($[O_2] = 0.35 – 2.20$ μmol.l^{-1}) suggesting that an oxygen threshold determines the
394 penetration of most megafaunal taxa into the OMZ (e.g., Murty et al., 2009). At the
395 800 m stations, peaks in megafaunal abundance were driven by high densities of
396 ophiuroids and decapod crustaceans. These abundance peaks are broadly consistent
397 with observations made on the OMZ-impacted margins (Smallwood et al., 1999;
398 Murty et al., 2009) but occur at shallower depths. Observed peaks in abundance at
399 800 m were lower than the 27.85 m^{-2} reported by Murty et al. (2009) at 1000 m on the
400 Pakistan margin, falling instead within the range of megafaunal densities in the
401 abyssal Arabian Sea (0.02 - 0.10 m^{-2}; Turnewitsch et al., 2000). Spatial patchiness and
402 artefacts in the experimental design make comparison of abundances by photographic
403 and video surveys challenging (Tessier et al., 2005). However, the observed
404 megafaunal abundance peaks on the Indian and Pakistan margins suggest that regional
405 differences in OMZ intensity between the two margins will have an important
406 influence upon the megafaunal assemblages.
407
408 Between 800 and 2000 m there was a decrease in megafaunal abundance and an
409 increase in the number of taxa. This is observed within the nMDS ordination as a
410 reduction in the distance between replicates (Fig. 6), indicative of a decrease in

411 community patchiness. These changes in the megafaunal assemblage are complex but
412 can be explained by the interactions between individual organisms and their
413 environments. Seven taxa were identified as important to megafaunal assemblage
414 structure, of which, three of these (actiniarians, ophiuroids and decapods) exhibited
415 strong correlations to the sediment C:N ratio. In contrast, the abundance of two
416 comparatively rare taxa, the asteroids and echinoids, correlated strongly with ambient
417 oxygen concentrations. These patterns may be explained by the specific behavioural
418 and physiological adaptations of each taxon to environmental hypoxia (reviewed by
419 Diaz and Rosenberg, 1995; Childress and Seibel, 1998). However, the results of the
420 present study support previous evidence that the specific responses of individual taxa
421 to oxygen limitation and organic matter availability determine megafaunal zonation
422 on an OMZ-impacted continental margin (e.g., Levin et al., 1991; Murty et al., 2009;
423 Sellanes et al., 2010).
424
425 *4.2.Implications for benthic ecosystem processes*
426
427 Changes in megafaunal assemblages across an OMZ are likely to have important
428 implications for benthic ecosystem processes. Megafauna directly contribute to
429 organic matter recycling by stripping labile organic matter from the sediment
430 (Smallwood et al., 1999; Jeffreys et al., 2009a) and reworking the sediment through
431 bioturbation. The megafauna also have indirect effects upon ecosystem processes
432 through predation and disturbance of meio- and macro-faunal taxa (Ambrose, 1993;
433 Hudson and Wigham, 2003). Megafaunal abundance and lebensspuren density are
434 correlated with bioturbation intensity (Turnewitsch et al., 2000; Wheatcroft, 2006)
435 and it is possible to infer megafaunal contributions to sediment reworking from this
436 data.
437
438 The absence of invertebrate megafauna and lebensspuren at the 540 m station,
439 suggests that megafaunal reworking of the sediment is minimal in the OMZ core.
440 However, the sparse fish fauna may be responsible for low levels of bioturbation,
441 since gobiid fishes were observed to bury themselves in the sediment (W.R. Hunter
442 and U. Witte, *pers. obs.*). In contrast, dense aggregations of small holes between 800
443 and 1100 m are characteristic of an infaunal ophiuroid assemblage (e.g., Solan and
444 Kennedy, 2002) coincident with recorded peaks in megafaunal abundance and

biomass. These observations suggest that the megafauna play an important role in the reworking of surficial sediments within the OMZ boundary. Results that are consistent with observations made at similar depths on the Oman and Pakistan margins (Smallwood et al. 1999; Jeffreys et al., 2009a). Between 1100 and 2000 m, there appear to be differences in sediment reworking that correspond to decreases in megafaunal abundance and biomass. Within this depth range observations of echiuran and enteropneust traces suggest that mega-infauna contribute to sediment mixing. In addition, deep scours in the sediment indicate that burrowing by fishes and crustaceans (Gaillard, 1991) provide pathways for mixing of surficial and deeper sediment layers. Thus, it can be inferred that megafaunal contributions to sediment reworking were minimal in the OMZ core and changed across the lower OMZ boundary, from reworking of surficial sediments (800 – 1100 m) to deeper mixing of the sediment between 1100 and 2000 m

4.4. Conclusions.

The epi-benthic megafaunal assemblage exhibits structural changes across the Indian margin OMZ. Invertebrate megafauna were absent from the OMZ core (540 m; $[O_2]$ = 0.35 $\mu mol.l^{-1}$), peaks in ophiuroid and decapod densities occurred at 800 m ($[O_2]$ = 2.2 - 2.36 $\mu mol.l^{-1}$) and megafaunal assemblage complexity increased across the lower OMZ boundary (800 – 2000 m). These faunal distributions are consistent with previous OMZ studies (Wishner et al., 1990; 1995; Murty et al., 2009; Sellanes et al., 2010) and suggest that the biofacies model of Levin et al. (1991) is an effective predictor of megafaunal zonation. The present study demonstrates that changes in megafaunal assemblage structure can be explained by correlations between the abundance of individual taxa, and both oxygen concentration and the sediment C:N ratio. This suggests that changes in megafaunal assemblage structure are dictated by oxygen and sediment organic matter limitation. The differences in megafaunal assemblage and lebensspuren across the OMZ suggest a changing role for the megafauna in sediment reworking and organic matter recycling, from low activity levels in the OMZ core, to higher levels both in the OMZ boundary (800 – 1100 m) and below the OMZ (2000 m). However, these conclusions are speculative and require further investigation using both empirical and modelling approaches.

5. Acknowledgements

The authors gratefully acknowledge the tireless efforts made by the officers and crew of both the R/V Yokosuka and Shinkai 6500 during YK08-11. We thank Dr Andy Gooday and three anonymous reviewers, whose constructive comments helped much improve this manuscript. We also thank the YK08-11 scientific team for their assistance during the cruise and Dr Waji Naqvi (NIO, India) for his assistance both pre- and post cruise. The authors acknowledge Dr Nikki King (U. Aberdeen) and Dr Matthias Stehman (ICTHYS) for their assistance in fish identification, and Miss Claire Mitchell for her assistance with the video analysis. The work was supported by the Carnegie Trust (United Kingdom) (grant no. ERI 008427 to U Witte), WRH was supported by a NERC Doctoral Training Grant (NE/G523904/1).

491 **6. References**

492 Ambrose, W.G. 1993. Effects of predation and disturbance by ophiuroids on soft-
493 bottom community structure in Oslofjord: Results of a mesocosm study. Mar. Ecol.
494 Prog. Ser. **97** (3): 225-236.

495 Anderson, M.J. 2006. Distance-based tests for homogeneity of multivariate
496 dispersions. Biometrics. **62** (1): 245-253.

497 Bakun, A., Weeks, S.J. 2004. Greenhouse gas buildup, sardines, submarine eruptions
498 and the possibility of abrupt degradation of intense marine upwelling ecosystems.
499 Ecol. Lett. **7**: 1015-1023.

500 Barriga, E., Salazar, C., Palacios, J., Romero, M., Rodríguez, A. 2009. Distribution,
501 abundance, and population structure of deep red shrimp *Haliporoides diomedeae*
502 (Crustacea: Decapoda: Solenoceridae) off northern Perú (2007-2008). Lat. Am. J. Aq.
503 Res. **37** (3): 371-380.

504 Billett, D.S.M., Bett, B.J., Jacobs, C.L., Rouse, I.P., Wigham, B.D. 2006. Mass
505 deposition of jellyfish in the deep Arabian Sea. Limnol. Oceanogr. **51** (5): 2077-2083.

506 Breitzke, M (2006). Physical properties of marine sediments. In: Schulz HD and
507 Zabel M (eds) Marine Geochemistry. 2nd ed. Springer-Verlag, Berlin, pp 28.

508 Childress, J.J., Seibel, B.A. 1998. Life at stable low oxygen levels: Adaptations of
509 animals to oceanic oxygen minimum layers. J. Exp. Biol. **201**: 1223-1232.

510 Christiansen, B., Beckmann, W., Weikert, H. 2001. The structure and carbon demand
511 of the bathyal benthic boundary layer community: A comparison of two oceanic
512 locations in the NE-Atlantic. Deep Sea Res. Part II. **48** (10): 2409-2424.

513 Clarke, K.R. 1993. Non-parametric multivariate analyses of changes in community
514 structure. Aust. J. Ecol. **18**: 117-143.

515 Cook, A.A., Lambshead, P.J.D., Hawkins, L.E., Mitchell, N., Levin, L.A. 2000.
516 Nematode abundance at the oxygen minimum zone in the Arabian Sea. Deep Sea Res.
517 Part II. **47** (1-2): 75-85.

518 Cowie, G.L., Calvert, S.E., Pedersen, T.F., Schulz, H., Von Rad, U. 1999. Organic
519 content and preservational controls in surficial shelf and slope sediments from the
520 Arabian Sea (Pakistan margin). Mar. Geol. **161** (1): 23-38.

521 Devol, A.H., Hartnett, H.E. 2001. Role of the oxygen-deficient zone in transfer of
522 organic carbon to the deep ocean. Limnol. Oceanogr. **46** (7): 1684-1690.

523 Diaz, R. J., Rosenberg, R. 1995. Marine benthic hypoxia: a review of its ecological
524 effects and the behavioral responses of benthic macrofauna. Oceanogr. Mar. Biol.
525 Ann. Rev. **33**: 245-303.

526 Gage, J.D. 2003. Growth and production of *Ophiocten gracilis* (Ophiuroidea:
527 Echinodermata) on the Scottish continental slope. Mar. Biol. **143** (1): 85-97.

528 Gaillard, C. 1991. Recent organism traces and ichnofacies on the deep-sea floor off
529 New Caledonia, Southwestern Pacific. Palaios. **6** (3): 302-315.

530 Gallucci, F., Fonseca, G., Soltwedel, T. 2008. Effects of megafauna exclusion on
531 nematode assemblages at a deep-sea site. Deep Sea Res. Part I. **55** (3): 332-349.

532 Ginger, M.L., Billett, D.S.M., Mackenzie, K.L., Kiriakoulakis, K., Neto, R.R.,
533 Boardman, D.K., Santos, V.L.C.S., Horsfall, I.M., Wolff, G.A. 2001. Organic matter
534 assimilation and selective feeding by holothurians in the deep sea: Some observations
535 and comments. Prog. Oceanogr. **50** (1-4): 407-421.

536 Gooday, A.J., Bernhard, J.M., Levin, L.A., Suhr, S.B. 2000. Foraminifera in the
537 Arabian Sea oxygen minimum zone and other oxygen-deficient settings: Taxonomic
538 composition, diversity, and relation to metazoan faunas. Deep Sea Res. Part II. **47** (1-
539 2): 25-54.

540 Grassle, J.F., Sanders, H.L., Hessler, R.R., Rowe, G.T., McLellan, T. 1975. Pattern
541 and zonation: A study of the bathyal megafauna using the research submersible *Alvin*..
542 Deep Sea Res. Part I. **22**: 457-481.

543 Hedges, J.I., Stern, J.H. 1984. Carbon and nitrogen determinations of carbonate-
544 containing solids. Limnol. Oceanogr. **29** (3): 657-663.

545 Hedges, J.I., Keil, R.G. 1995. Sedimentary organic matter preservation: An
546 assessment and speculative synthesis. Mar. Chem. **49** (2-3): 81-115.

547 Helly, J.J., Levin, L.A. 2004. Global distribution of naturally occurring marine
548 hypoxia on continental margins. Deep Sea Res. Part I. **51** (9): 1159-1168.

549 Hudson, I.R., Wigham, B.D. 2003. *In situ* observations of predatory feeding
550 behaviour of the galatheid squat lobster *Munida sars*i using a remotely operated
551 vehicle. J. Mar. Biol. Assoc. U. K. **83** (3): 463-464.

552 Jeffreys, R.M., Wolff, G.A., Cowie, G.L. 2009a. Influence of oxygen on heterotrophic
553 reworking of sedimentary lipids at the Pakistan Margin. Deep Sea Research Part II:
554 Topical Studies in Oceanography. **56** (6-7): 358-375.

555 Jeffreys, R.M., Wolff, G.A., Murty, S.J. 2009b. The trophic ecology of key
556 megafaunal species at the Pakistan margin: Evidence from stable isotopes and lipid
557 biomarkers. Deep-Sea Research Part I: Oceanographic Research Papers. **56** (10):
558 1816-1833.

559 Jones, D.O.B., Bett, B.J., Tyler, P.A. 2007. Megabenthic ecology of the deep Faroe-
560 Shetland channel: A photographic study. Deep Sea Res. Part I. **54** (7): 1111-1128.

561 Kimmel, J.J. 1985. A new species-time method for visual assessment of fishes and its
562 comparison with established methods. Env. Biol. Fish. **12** (1): 23-32.

563 Kitchell, J.A., Kitchell, J.F., Clark, D.L., Dangeard, L. 1978. Deep-sea foraging
564 behavior: Its bathymetric potential in the fossil record. Science. **200** (4347): 1289-
565 1291.

566 Lampitt, R.S., Billett, D.S.M., Rice, A.L. 1986. Biomass of the invertebrate
567 megabenthos from 500 to 4100 m in the northeast Atlantic Ocean. Mar. Biol. **93** (1):
568 69-81.

569 Levin, L.A. 2003. Oxygen minimum zone benthos: Adaptation and community
570 response to hypoxia. Oceanogr. Mar. Biol. Ann. Rev. **41**: 1-45.

571 Levin, L.A., Huggett, C.L., Wishner, K.F. 1991. Control of deep-sea benthic
572 community structure by oxygen and organic-matter gradients in the eastern Pacific
573 Ocean. J. Mar. Res. **49** (4): 763-800.

574 Mauviel, A., Kim Juniper, S., Sibuet, M. 1987. Discovery of an enteropneust
575 associated with a mound-burrows trace in the deep sea: Ecological and geochemical
576 implications. Deep Sea Res. Part I. **34** (3): 329-335.

577 Michelland, R., Cauquil, L. 2010. StatFingerprints. **2.0**.

578 Miller, R.J., Smith, C.R., DeMaster, D.J., Fornes, W.L. 2000. Feeding selectivity and
579 rapid particle processing by deep-sea megafaunal deposit feeders: A ^{234}Th tracer
580 approach. J. Mar. Res. **58** (4): 653-673.

581 Murty, S.J., Bett, B.J., Gooday, A.J. 2009. Megafaunal responses to strong oxygen
582 gradients on the Pakistan margin of the Arabian Sea. Deep Sea Res. Part II. **56** (6-7):
583 472-487.

584 Ohta, S. 1984. Star-shaped feeding traces produced by echiuran worms on the deep-
585 sea floor of the Bay of Bengal. Deep Sea Res. Part I. **31** (12): 1415-1432.

586 Oksanen, J., Kindt, R., Legendre, P., O'Hara, B., Simpson, G.L., Solymos, P.M.,
587 Stevens, H.H., Wagner, H. 2009. Vegan: Community ecology package. **1.15-4**.

588 Piepenburg, D., Schmid, M.K. 1996. Brittle star fauna (Echinodermata: Ophiuroidea)
589 of the Arctic northwestern Barents Sea: Composition, abundance, biomass and spatial
590 distribution. Polar Biol. **16** (6): 383-392.

591 Piepenburg, D., Blackburn, T.H., von Dorrien, C.F., Gutt, J., Hall, P.O., Hulth, S.,
592 Kendall, M.A., Opalinski, K.W., Rachor, E., Schmid, M.K. 1995. Partitioning of
593 benthic community respiration in the Arctic (northwestern Barents Sea). Mar. Ecol.
594 Prog. Ser. **118** (1-3): 199-214.

595 Quiroga, E., Sellanes, J., Arntz, W.E., Gerdes, D., Gallardo, V.A., Hebbeln, D. 2009.
596 Benthic megafaunal and demersal fish assemblages on the Chilean continental

margin: The influence of the oxygen minimum zone on bathymetric distribution. Deep Sea Res. Part II. **56** (16): 1061-1072.

R Development Core Team. 2009. R: A language and environment for statistical computing. R Foundation for Statistical Computing.

Renaud, P.E., Morata, N., Ambrose, W.G., Bowie, J.J., Chiuchiolo, A. 2007. Carbon cycling by seafloor communities on the eastern Beaufort Sea shelf. J. Exp. Mar. Biol. Ecol. **349** (2): 248-260.

Sayer, M.D.J., Poonian, C. 2007. The influences of census technique on estimating indices of macrofaunal population density in the temperate rocky subtidal zone. Und. Tech. **27**: 119-139.

Schmaljohann, R., Drews, M., Walter, S., Linke, P., Von Rad, U., Imhoff, J.F. 2001. Oxygen-minimum zone sediments in the northeastern Arabian Sea off Pakistan: A habitat for the bacterium *Thioploca*. Mar. Ecol. Prog. Ser. **211**: 27-42.

Sellanes, J., Neira, C., Quiroga, E., Teixido, N. 2010. Diversity patterns along and across the Chilean margin: A continental slope encompassing oxygen gradients and methane seep benthic habitat. Mar. Ecol. Evol. Appr. **31** (1): 111-124.

Smallwood, B.J., Wolff, G.A., Bett, B.J., Smith, C.R., Hoover, D., Gage, J.D., Patience, A. 1999. Megafauna can control the quality of organic matter in marine sediments. Naturwissenschaften. **86** (7): 320-324.

Solan, M., Kennedy, R. 2002. Observation and quantification of *in situ* animal-sediment relations using time-lapse sediment profile imagery (t-SPI). Mar. Ecol. Prog. Ser. **228**: 179-191.

Solan, M., Germano, J.D., Rhoads, D.C., Smith, C., Michaud, E., Parry, D., Wenzhöfer, F., Kennedy, B., Henriques, C., Battle, E., Carey, D., Iocco, L., Valente, R., Watson, J., Rosenberg, R. 2003. Towards a greater understanding of pattern, scale and process in marine benthic systems: A picture is worth a thousand worms. J. Exp. Mar. Biol. Ecol. **285-286**: 313-338.

624 Spearman, C. 1904. The proof and measurement of association between two things.
625 Amer. J. Psych. **15** (1): 72-101.

626 Stevens, H., Ulloa, O. 2008. Bacterial diversity in the oxygen minimum zone of the
627 eastern tropical South Pacific. Environ. Microbiol. **10** (5): 1244-1259.

628 Stramma, L., Johnson, G.C., Sprintall, J., Mohrholz, V. 2008. Expanding oxygen-
629 minimum zones in the tropical oceans. Science. **320** (5876): 655-658.

630 Tessier, E., Chabanet, P., Pothin, K., Soria, M., Lasserre, G. 2005. Visual censuses of
631 tropical fish aggregations on artificial reefs: Slate versus video recording techniques.
632 J. Exp. Mar. Biol. Ecol. **315** (1): 17-30.

633 Thurston, M.H., Bett, B.J., Rice, A.L., Jackson, P.A.B. 1994. Variations in the
634 invertebrate abyssal megafauna in the North Atlantic Ocean. Deep Sea Res.Part I. **41**
635 (9): 1321-1348.

636 Turnewitsch, R., Witte, U., Graf, G. 2000. Bioturbation in the abyssal Arabian sea:
637 Influence of fauna and food supply. Deep Sea Res. Part II. **47**: 2877-2911.

638 Uchida, H., Takeshi, K., Ikuo, K., Masao, F. 2008. *In situ* calibration of optode-based
639 oxygen sensors. J. Atmos. Oceanic Technol. **25**: 2271-2281.

640 Vandewiele, S., Cowie, G., Soetaert, K., Middelburg, J.J. 2009. Amino acid
641 biogeochemistry and organic matter degradation state across the Pakistan margin
642 oxygen minimum zone. Deep Sea Res. Part II. **56** (6-7): 376-392.

643 Venables, W.N., Ripley, B.D. 2002. Modern applied statistics with S. Springer, New
644 York.

645 Wheatcroft, R.A. 2006. Time-series measurements of macrobenthos abundance and
646 sediment bioturbation intensity on a flood-dominated shelf. Prog. Oceanogr. **71** (1):
647 88-122.

648 Wishner, K., Levin, L., Gowing, M., Mullineaux, L. 1990. Involvement of the oxygen
649 minimum zone in benthic zonation on a deep seamount. Nature. **346** (6279): 57-59.

650 Wishner, K.F., Ashjian, C.J., Gelfman, C., Gowing, M.M., Kann, L., Levin, L.A.,
651 Mullineaux, L.S., Saltzman, J. 1995. Pelagic and benthic ecology of the lower
652 interface of the eastern tropical Pacific oxygen minimum zone. Deep Sea Res. Part I.
653 **42** (1): 93-115.

654 Witte, U. 1999. Consumption of large carcasses by scavenger assemblages in the deep
655 Arabian Sea: Observations by baited camera. Mar. Ecol. Prog. Ser. **183**: 139-147.

656 Woulds, C., Cowie, G.L. 2009. Sedimentary pigments on the Pakistan margin:
657 Controlling factors and organic matter dynamics. Deep Sea Res. Part II. **56** (6-7): 347-
658 357.

659 Zuur, A.F., Ieno, E.N., Elphick, C.S. 2010. A protocol for data exploration to avoid
660 common statistical problems. Meth. Ecol. Evol. **1** (1): 3-14.

Table Legends

Table 1: Video survey and environmental parameters at each of the six survey stations, identified by transect (T1 or T2) and depth. Surficial sediment characteristics include total organic carbon content (% TOC), total nitrogen content (% TN) and the carbon-nitrogen ratio (C:N ratio).

Table 2: The 13 main megafaunal groups counted during the video surveys and taxa identified within each group by *post-hoc* image analysis.

Table 3: Lebensspuren groups counted during video surveys.

Table 4: Megafaunal abundance data (m^{-2}) calculated from video surveys, at six stations spanning the Indian margin OMZ. Data are mean values (± standard deviation) of *n* replicate surveys.

Table 5: Correlations between megafaunal abundances and the main environmental parameters across the Indian margin OMZ. Data are displayed as Spearman's Rank correlation co-efficient (ρ_s) and p-values. Statistically significant values are highlighted in bold font..

Figure Legends

Fig. 1: Bathymetric map of the study area. Contours represent 200 m depth intervals, 1000 m intervals are highlighted in bold.

Fig. 2: Oxygen, temperature and salinity profiles recorded using an optode mounted upon *Shinkai 6500* during *YK08-11*. Dashed lines represent the zonation of the OMZ, as described by Levin (2003).

Fig 3. Paired scatterplots showing the relationship (top-right) and correlation strength (bottom-left) between all environmental variables measured in the present study. Correlation strengths are displayed as Spearman's Rank Correlation Coefficients, with the size of each number representing the relative correlation strength.

Fig. 4: Representative images of the sediment surface at each survey station showing (A) snailfish (Liparidae spp.) and (B) rippled sediment at T1 540 m; C) brittlestars (*Ophiolimna* spp.) at T1 800 m; (D) a Brisingid sea star (Brisingida spp.) and flytrap anemone (*Actinoscypha* spp.) at T1 1100 m; (E) a skate (*Bathyraja* spp.) and F) a scour (Lebensspuren) and sea star (Asteroidea spp.) at T1 2000 m; (G) Brittlestars (*Ophiolimna* spp.) and evidence of burrows at T2 800 m; (H) fish (*Coryphaenoides* spp.) and urchin (Echinoidea spp.) at T2 1100 m.

Fig. 5: Mean lebensspuren densities (± standard deviation) at the six survey stations.

Fig. 6: nMDS ordination of the variation in megafaunal assemblages across the six survey stations, calculated from Bray-Curtis dissimilarity indices at each station. Stations are displayed as symbols: T1 540 m (○); T1 800 m (Δ); T1 1100 m (□); T1 2000 m (+); T2 800 m (▲); T2 1100 m (■)

Fig. 7: Relative abundance (m^{-2}) of (A) the total megafaunal assemblage; (B) Actiniaria; (C) Decapoda; (D) Ophiuroidea; (E) Asteroidea; (F) Holothuroidea; (G) Echinoidea; (H) Gnathostomata; and (I) other taxa, at the six survey stations.

Fig. 8: Wet biomass estimates for ophiuroids and decapods at the six survey stations.

Appendix Legends

Appendix A: SIMPER Results: Average similarity in megafaunal assemblage structure between replicate surveys conducted at each station, and taxonomic groups contributing to 90% of this similarity.

Appendix B: SIMPER results II: Similarity matrix, detailing the taxonomic groups responsible for 90% of the cumulative difference in megafaunal assemblage structure between survey stations.

Appendix C: Biomass-frequency histograms for (A) ophiuroids and (B) decapods on the Indian margin OMZ.

727 Table 1.

Station	Mean Area Surveyed (m^2)	Mean Water Depth (m)	Water Physico-chemistry			Surficial Sediment Characteristics (0-1cm)			
			O_2 ($\mu mol.l^{-1}$)	Temp. (^oC)	Salinity (‰)	% TOC	% TN	C:N ratio	Porosity ϕ
T1 530 m	58.75 (±5.09)	540	0.35	12.1	35.2	1.84 (±0.33)	0.19 (±0.04)	9.72 (±0.20)	72.25 (±1.25)
T1 800 m	52.30 (±3.45)	800	2.20	10.1	35.1	2.12 (±1.03)	0.23 (±0.09)	8.94 (±1.11)	74.96 (±0.65)
T1 1100 m	56.40 (±5.84)	1100	15.00	9.2	35.0	2.59	0.27	9.57	77.44
T1 2000 m	53.39 (±7.14)	2000	136.00	2.8	34.5	1.21 (±0.12)	0.06 (±0.01)	19.38 (±1.84)	68.32 (±0.82)
T2 800 m	58.34 (±4.82)	800	2.36	9.9	35.1	3.20 (±0.85)	0.38 (±0.12)	8.41 (±0.43)	74.93 (±1.93)
T2 1100 m	80.20 (±9.27)	1100	15.00	7.2	34.8	2.41(±0.95)	0.29 (±0.11)	8.38 (±0.62)	80.19 (±1.44)

728 Table 2.

Phylum	Taxonomic Groups Surveyed	Identified Taxa
Porifera	Whole Phylum	Hexactinellida spp.
		Demospongia spp.
Cnidaria	Actiniaria	Actiniaria spp.
		Actinoscyphia spp.
	Pennatulacea	Pennatulacea spp.
Mollusca	Bivalvia	Pectenidea spp.
	Gastropoda	Gastropoda spp.
Arthropoda	Decapoda	*Plesiopenaeus* spp.
		Solenocera spp.
		Encephaloides spp.
	Iospoda	*Bathynomus* spp.
Echinodermata	Ophiuroidea	*Ophiolimna* spp.
		Amphiura spp.
	Asteroidea	Asteroidea spp.
		Brisingida spp.
	Holothuroidea	Holothuroidea spp.
		Mesothuria spp.
	Echinoidea	Echinoidea spp.
Chordata	Ascidiacea	Ascidiacea spp.
	Gnathostomata	Liparidae spp.
		Holcomycteronus spp.
		Coryphaenoides spp.
		Gobiidae spp.
		Congridae spp.
		Synaphobranchus spp.
		Etmopterus spp.
		Bathyraja spp.

729

730 Table 3.

Trace Type	**Description**
Locomotion Trail	Linear trace on the sea-floor made by the movement of an epi-faunal or semi-infaunal animal. Most probably produced by the feeding and movements of holothurians or echinoids.
Holes	Burrow openings on the sediment surface. They may occur both as singular and grouped into irregular clusters.
Hole Ring	Ring of 8 – 20 burrow openings arranged in a circle. These may surround a sediment mound or a central burrow opening. Identified as an enteropneust lebensspur (Mauviel, et al 1987).
Star-like Trace	Burrow hole surrounded by epichnial grooves, radiating outwards. Ascribed to the presence of a surface deposit feeding echiuran worm (Ohta 1984)
Scour	Linear depression (20 – 50 cm length) within the sea floor, bordered by a rim of raised sediment. Probably formed by fish or crustacea excavating the sediment.

731 Table 4

Station	**T1 540 m**	**T1 800 m**	**T1 1100 m**	**T1 2000 m**	**T2 800 m**	**T2 1100 m**
Replicates	*n = 4*	*n = 3*	*n = 3*	*n = 3*	*n = 3*	*n = 3*
Porifera		0.0007 *(±0.0013)*			0.0066 *(±0.0063)*	
Actiniaria		0.0991 *(±0.0656)*	0.0817 *(±0.0416)*	0.0106 *(±0.0056)*	0.0392 *(±0.0072)*	0.0709 *(±0.0181)*
Pennatulacea		0.0145 *(±0.0073)*	0.0027 *(±0.0010)*	0.0026 *(±0.0007)*	0.0031 *(±0.0054)*	0.0011 *(±0.0018)*
Bivalvia				0.0036 *(±0.0037)*	0.0010 *(±0.0018)*	0.0049 *(±0.0190)*
Gastropoda					0.0012 *(±0.0021)*	
Decapoda		0.1158 *(±0.0513)*	0.0363 *(±0.0096)*	0.0080 *(±0.0055)*	0.1480 *(±0.0107)*	0.0373 *(±0.0176)*
Isopoda			0.0024 *(±0.0016)*			
Asteroidea			0.0058 *(±0.0071)*			0.0099 *(±0.0099)*
Ophiuroidea		0.4430 *(±0.4250)*	0.0374 *(±0.0276)*	0.0005 *(±0.0009)*	0.2073 *(±0.1604)*	0.0173 *(±0.0150)*
Holothuroidea						0.0148 *(±0.0055)*
Echinoidea		0.0032 *(±0.0039)*	0.0046 *(±0.0046)*	0.0053 *(±0.0031)*		0.0151 *(±0.0043)*
Crinoidea		0.0084 *(±0.0097)*			0.0048 *(±0.0083)*	0.0008 *(±0.0014)*
Ascidiacea					0.0046 *(±0.0039)*	0.0030 *(±0.0051)*
Gnathostomata	0.0267 *(±0.0388)*	0.0529 *(±0.0476)*	0.0672 *(±0.0040)*	0.0055 *(±0.0018)*	0.0623 *(±0.0157)*	0.0426 *(±0.0140)*
Total Abundance	0.0267 *(±0.0039)*	0.7390 *(±0.3940)*	0.2380 *(±0.1489)*	0.0367 *(±0.0167)*	0.4780 *(±0.3130)*	0.2177 *(±0.0843)*

732 Table 5.

	Oxygen		C:N Ratio	
	ρ_s	p-value	ρ_s	p-value
Actiniaria	0.27	0.27	**-0.55**	**0.01**
Decapoda	0.16	0.52	**-0.62**	**<0.01**
Ophiuroidea	-0.06	0.82	**-0.56**	**0.01**
Asteroidea	**0.51**	**0.02**	-0.18	0.45
Echinoidea	**0.63**	**<0.01**	-0.26	0.29
Gnathostomata	-0.31	0.20	-0.44	0.06
Other Taxa	0.16	0.52	**-0.59**	**<0.01**
Total Megafaunal Abundance	<-0.01	0.99	**-0.68**	**<0.01**

733 Figure 1.

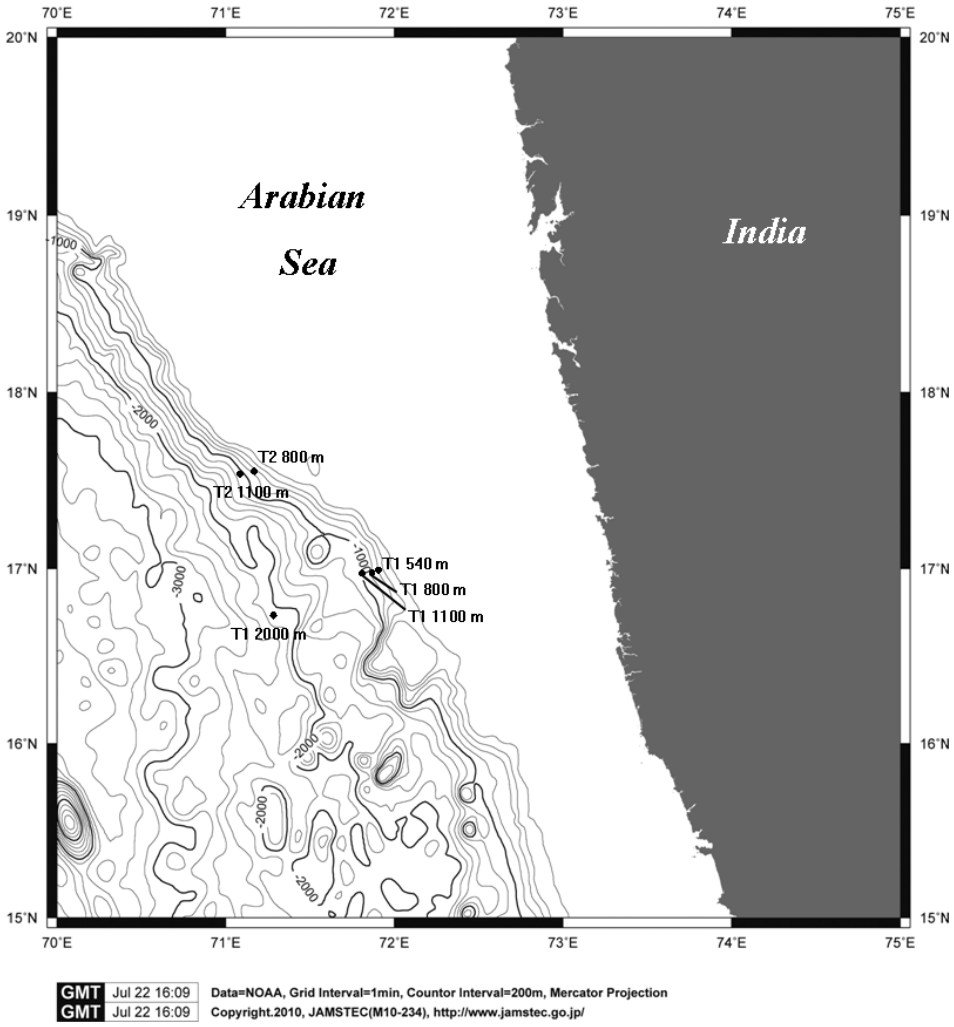

734

735 Figure 2

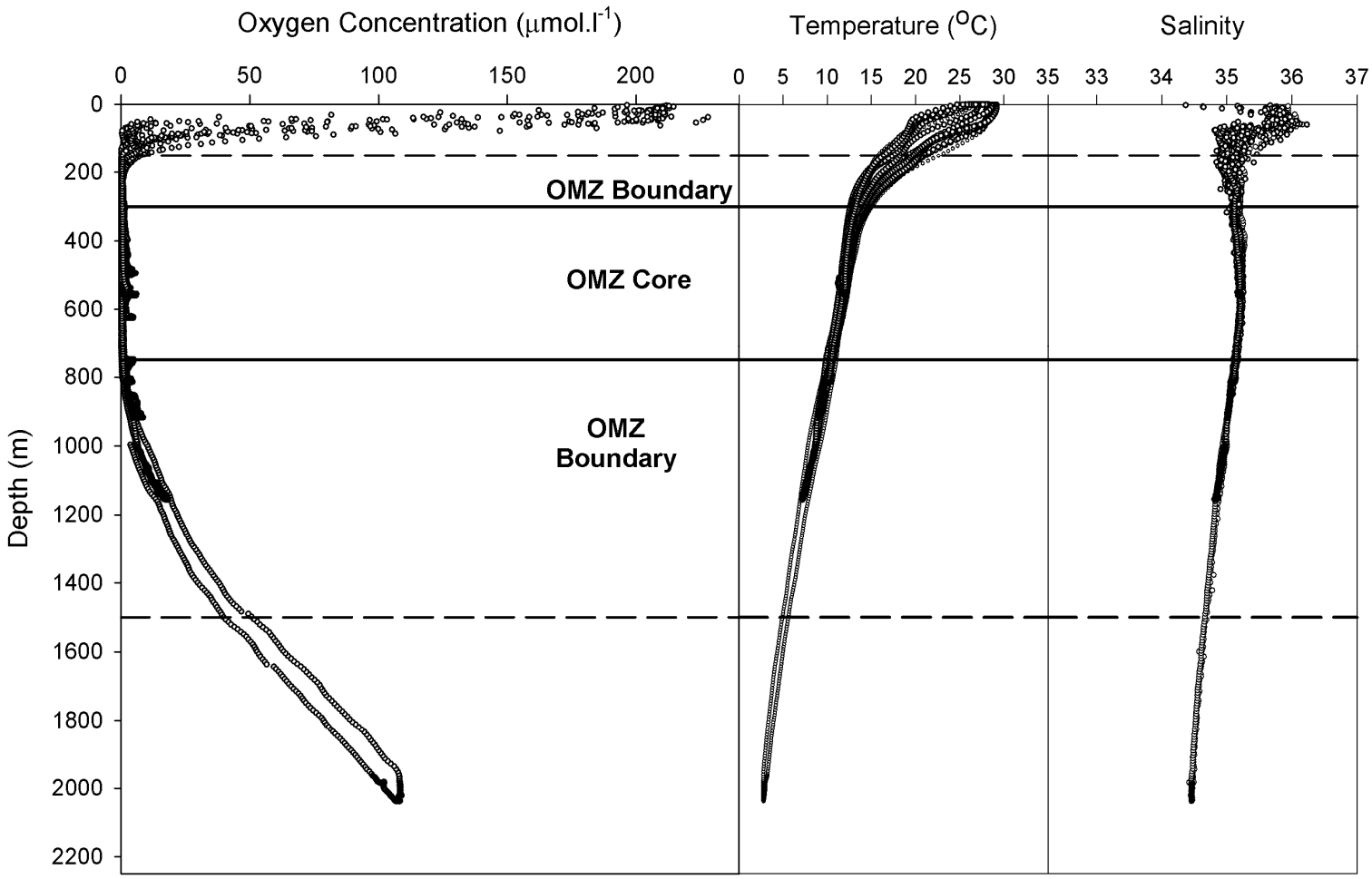

736

737 Figure 3.

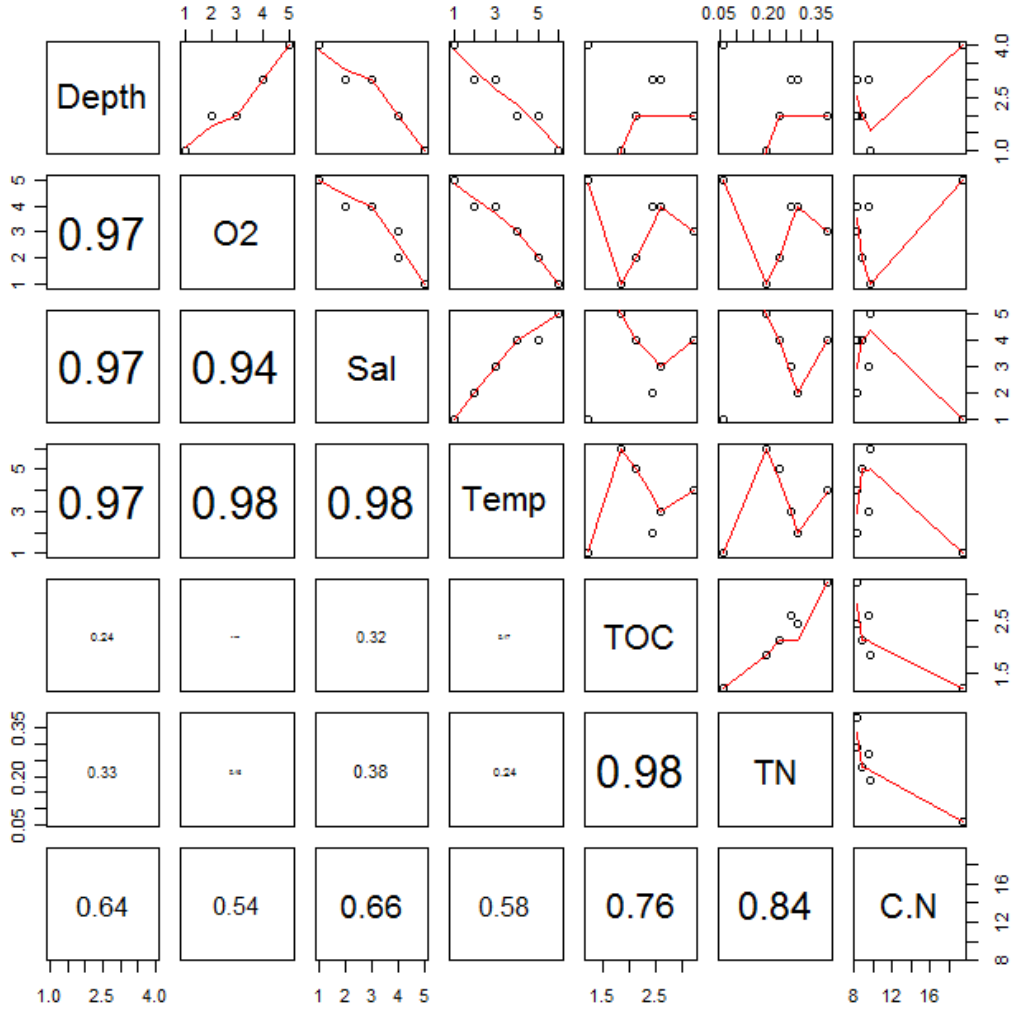

738

739 Figure 4.

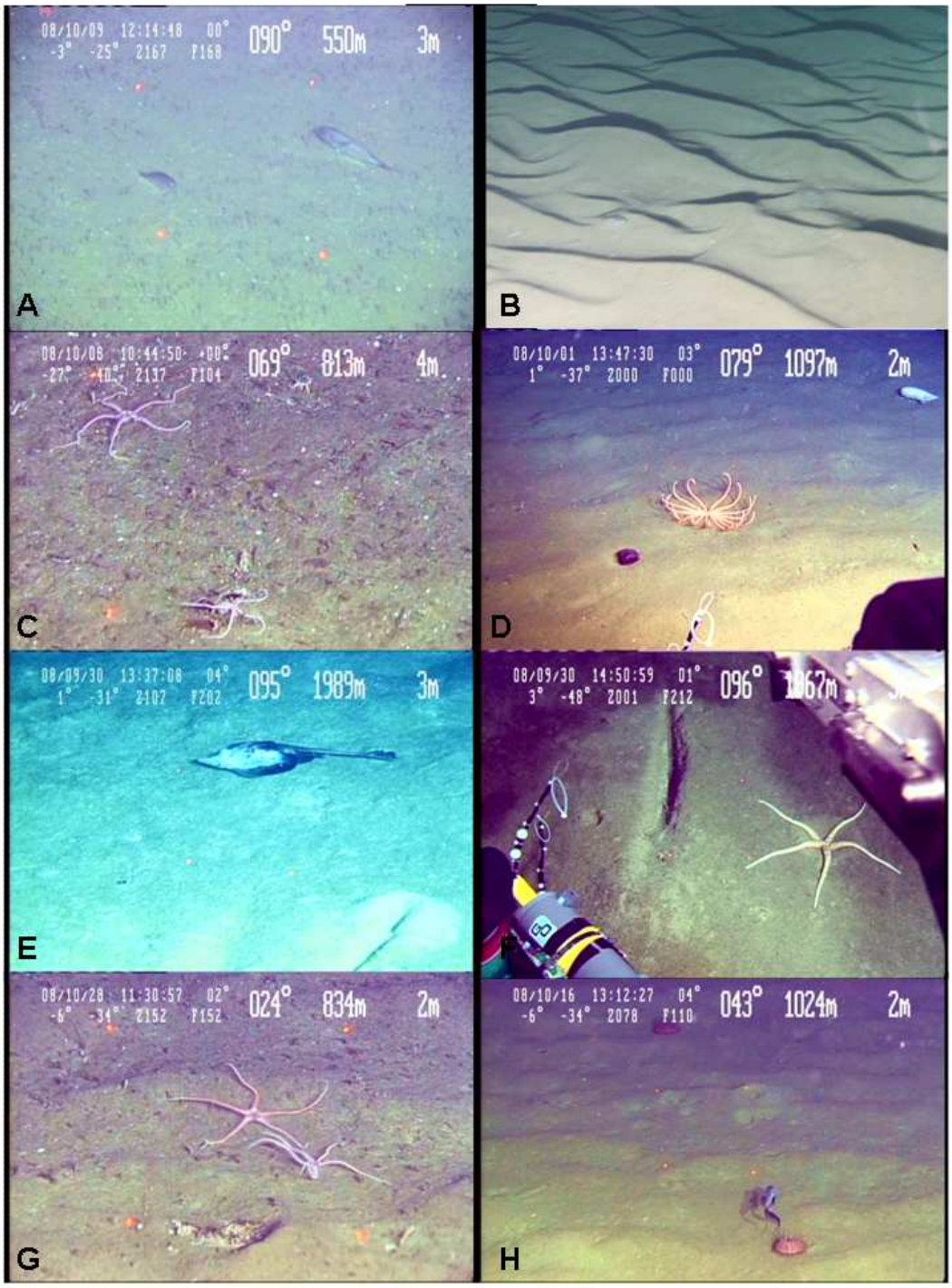

740

741 Figure 5

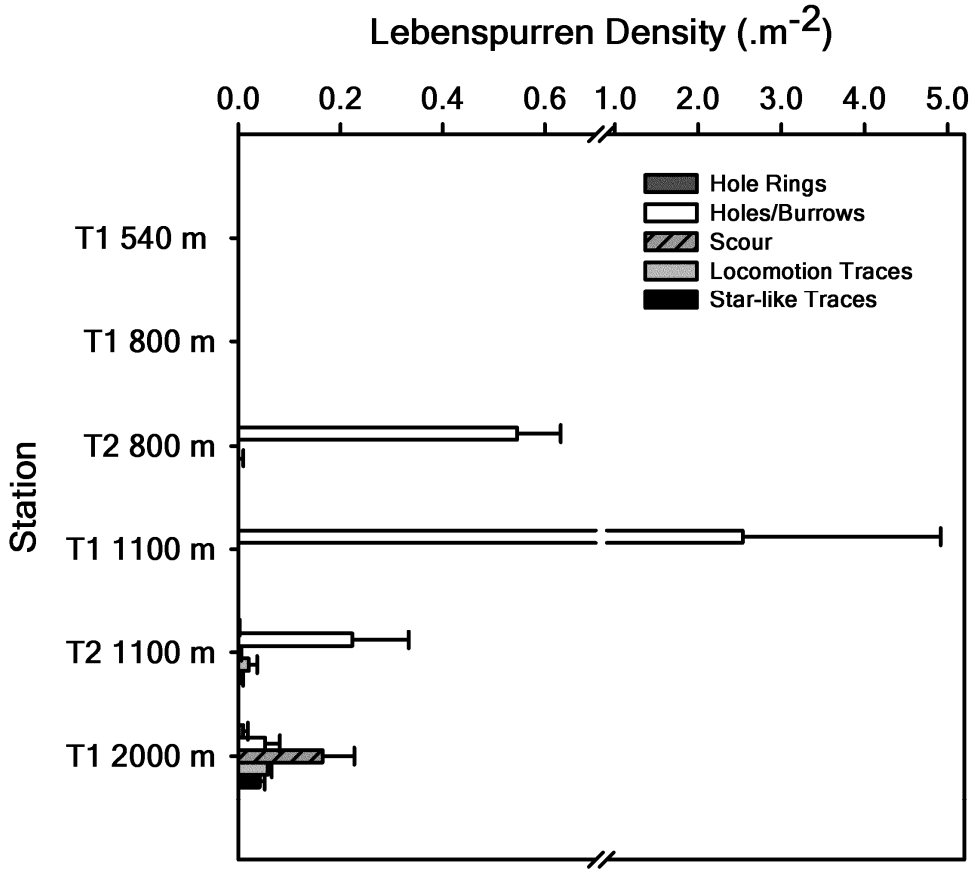

742

743 Figure 6.

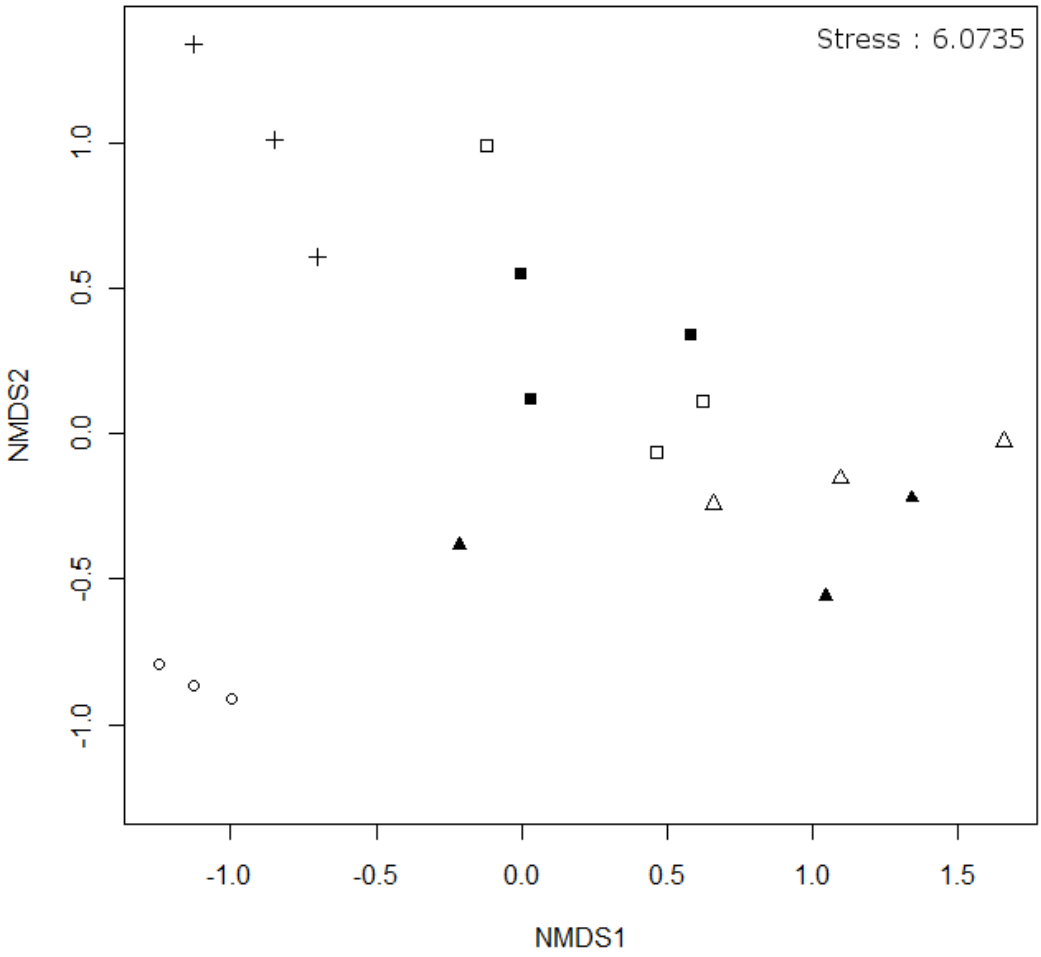

744

745 Figure 7.

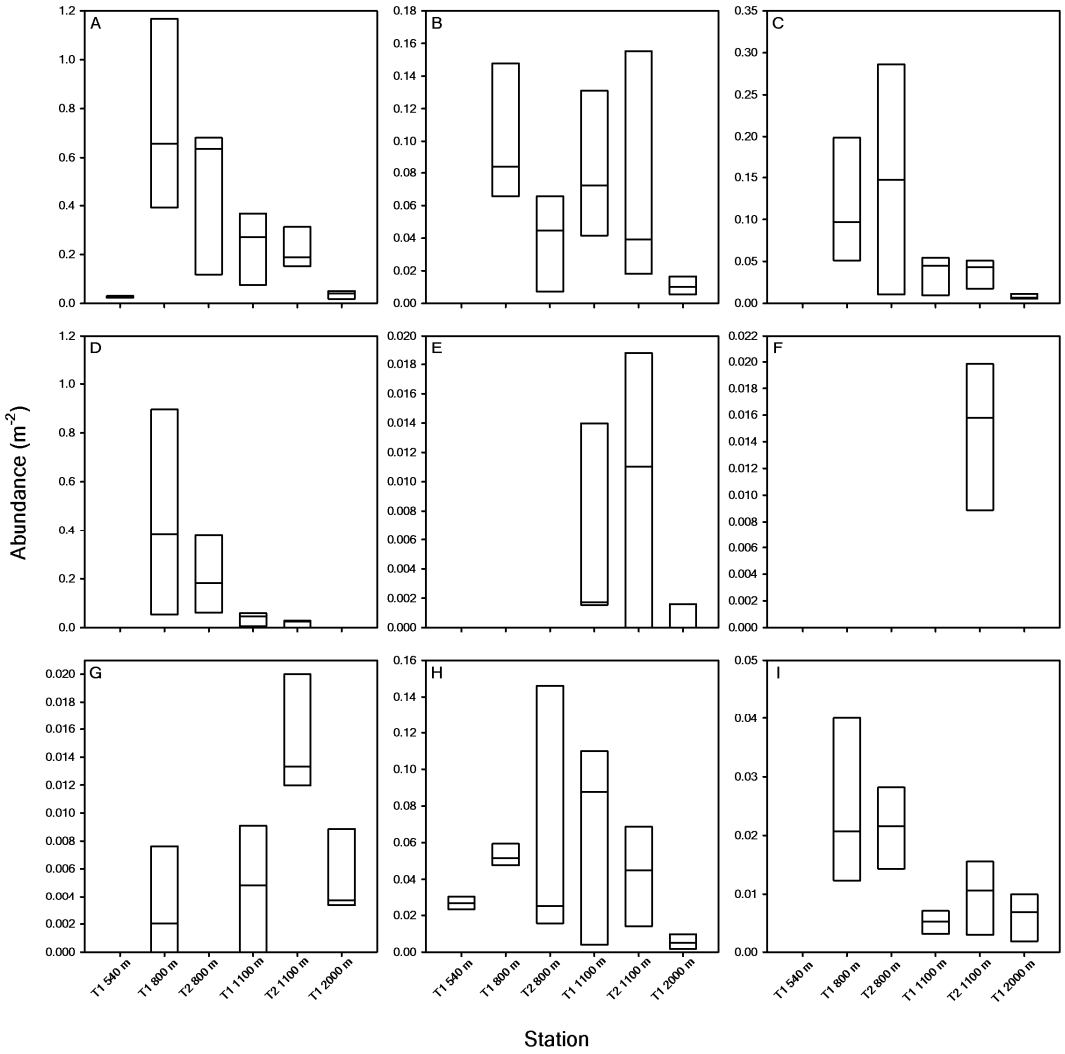

746

747 Figure 8.

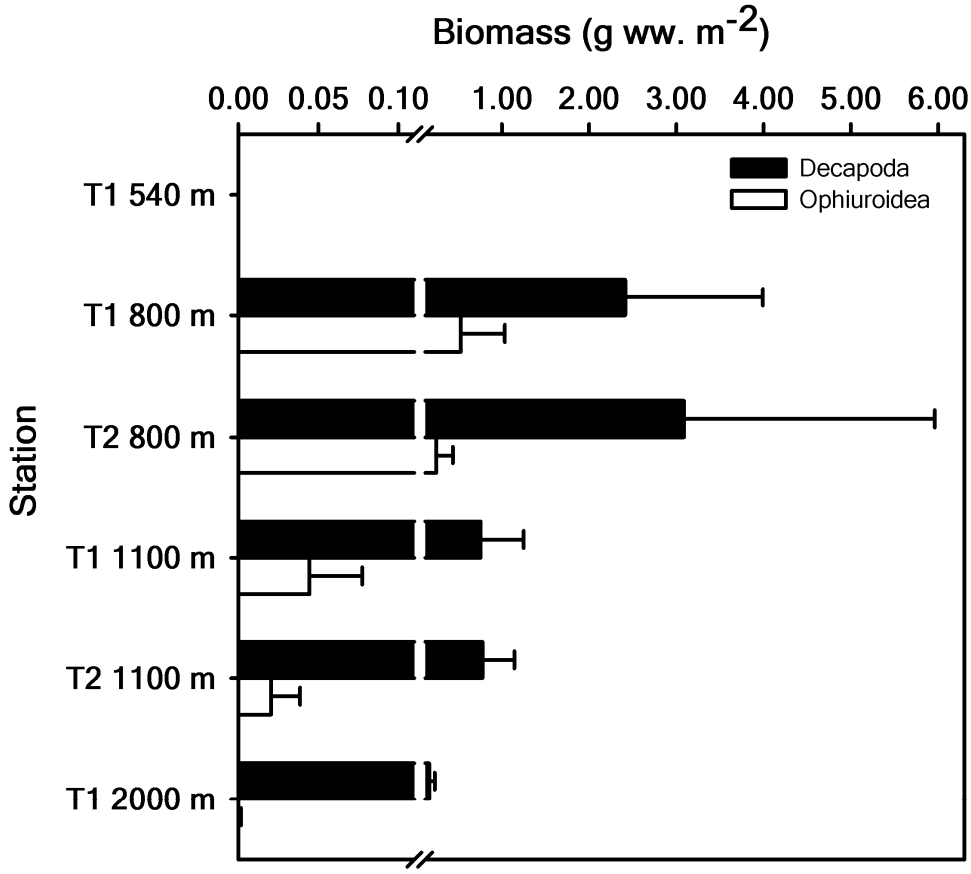

748

749 Appendix A.

Station	Average Similarity (%)	Contributing Taxa	Percentage Contribution (%)
T1 540 m	90.97	Gnathostomata	100.00
T1 800 m	48.70	Ophiuroidea	40.24
		Decapoda	21.03
		Actiniaria	20.62
		Gnathostomata	14.32
T1 1100 m	49.94	Actiniaria	43.71
		Gnathostomata	21.03
		Decapoda	15.95
		Ophiuroidea	14.06
T1 2000 m	60.71	Actiniaria	30.91
		Decapoda	27.27
		Echinoidea	16.10
		Gnathostomata	12.29
		Pennatulacea	9.31
T2 800 m	37.45	Ophiuroidea	52.58
		Decapoda	24.83
		Gnathostomata	11.40
		Actiniaria	9.35
T2 1100 m	53.97	Decapoda	21.77
		Actinaria	21.44
		Gnathostomata	19.89
		Echinoidea	10.84
		Holothuroidea	10.29
		Ophiuroidea	8.70

Appendix B.

	T1 540 m	T1 800 m	T1 1100 m	T1 2000 m	T2 800 m	T2 1100 m
T1 540 m		Ophiuroidea (52.19%) Decapoda (24.02%) Actiniaria (14.67%)	Actiniaria (37.73%) Gnathostomata (24.47%) Decapoda (14.67%) Ophiuroidea (14.56%)	Gnathostomata (43.20%) Aciniaria (19.20%) Decapoda (14.82%) Echinoidea (10.17%) Bivalvia (6.16%)	Ophiuroidea (49.18%) Decapoda (27.58%) Actiniaria (8.34%) Gnathostomata (8.13%)	Actiniaria (31.20%) Decapoda (18.50%) Gnathostomata(11.50%) Ophiuroidea (10.98%) Holothuroidea (8.64%) Echinoidea (8.48%) Asteroidea (6.12%)
T1 800 m			Ophiuroidea (57.57%) Decapoda (19.82%) Gnathostomata (8.99%) Aciniaria (7.53%)	Ophiuroidea (51.90%) Decapoda (22.40%) Actiniaria (12.77%) Gnathostomata (8.27%)	Ophiuroidea (51.63%) Decapoda (22.17%) Actiniaria (10.75%) Gnathostomata (9.05%)	Ophiuroidea (55.86%) Decapdoa (17.65%) Actiniaria (10.86%) Gnathostomata (3.91%) Holothuroidea (2.71%)
T1 1100 m				Actiniaria (36.6%) Gnathostomata (25.73%) Ophiuroidea (16.72%) Decapoda (12.24%)	Ophiuroidea (35.25%) Decapoda (24.90%) Gnathostomata (16.07%) Actiniaria (14.40%)	Actiniaria (27.16%) Gnathostomata (24.32%) Ophiuroidea (13.61%) Decapoda (10.51%) Holothuroidea (8.19%) Echinoidea (5.21%) Asteroidea (4.93%)
T1 2000 m					Ophiuroidea (46.73%) Decapoda (23.86%) Gnathostomata (13.15%) Actiniaria (6.11%) Crinoidae (3.60%)	Actiniaria (27.81%) Gnathostomata (18.73%) Decapoda (15.45%) Ophiuroidea (11.64%) Holothuroidea (9.30%) Asteroidea (6.43%) Echinoidea (6.07%)
T2 800 m						Ophiuroidea (35.62%) Decapoda (23.47%) Actiniaria (13.42%) Gnathostomata (10.54%) Holothuroidea (4.03%) Echinoidea (4.02%)

752 Appendix C.

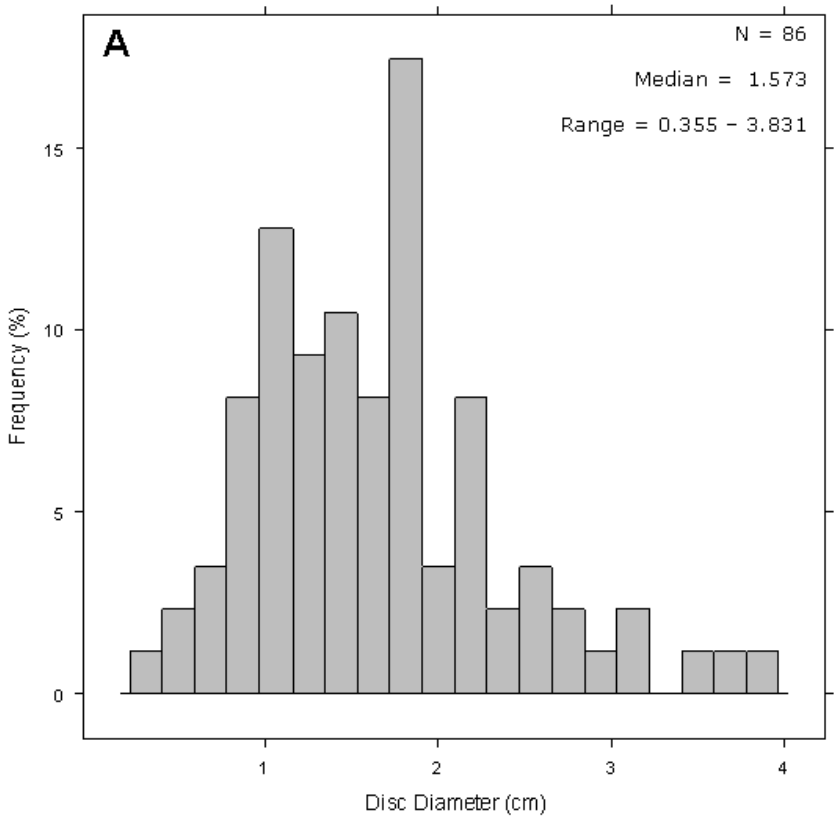

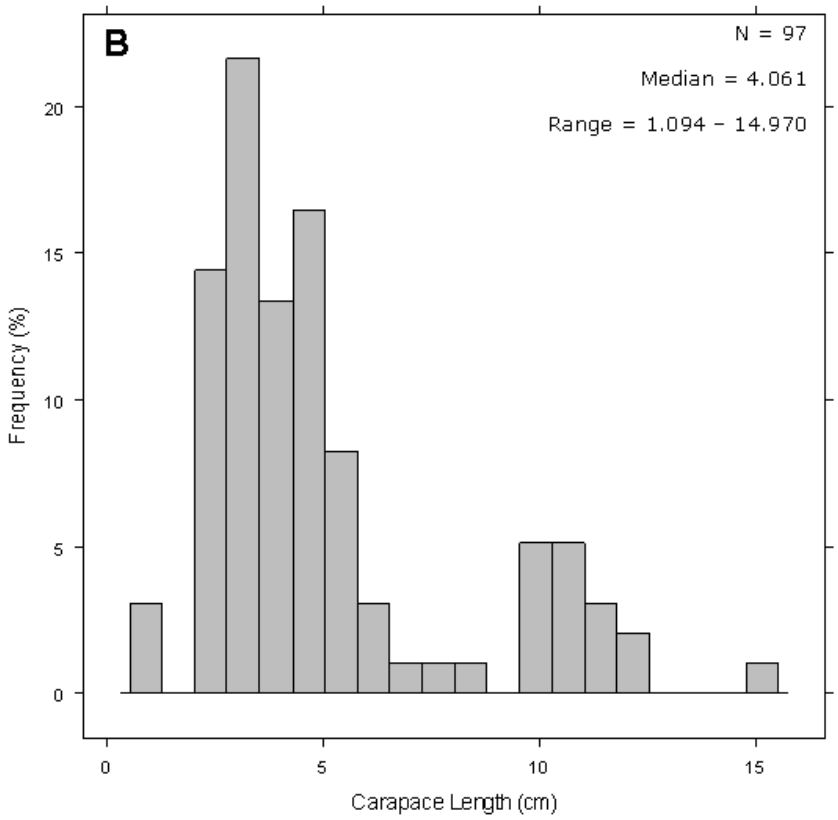

753